

A three-dimensional metal grid mesh as a practical alternative to ITO

Sungwoo Jang,^a Woo-Bin Jung,^a Choelgyu Kim,^c Phillip Won,^d Sang-Gil Lee,^a Kyeong Min Cho,^a Ming Liang Jin,^a Cheng Jin An,^a Hwan-Jin Jeon,^a Seung Hwan Ko,^d Taek-Soo Kim^c and Hee-Tae Jung^{a,b,*}

^aDepartment of Chemical and Biomolecular Engineering and ^bKAIST Institute for the NanoCentury, ^cDepartment of Mechanical Engineering, Korea Advanced Institute of Science and Technology (KAIST), 291 Daehak-ro, Yuseong-gu, Daejeon, 305-701, Republic of Korea

^dDepartment of Mechanical Engineering, Seoul National University, 1 Gwanak-ro, Gwanak-gu, Seoul, 151-742, Republic of Korea

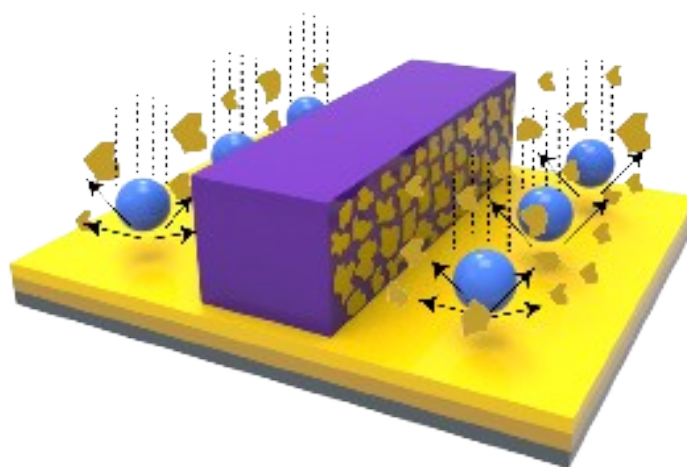


Figure S1. Schematic illustration of the secondary sputtering phenomenon (SSP). Note the deposition on the sidewall of the resist of particles ejected from a target material under Ar⁺ ion bombardment, which enables the fabrication of a metal nanostructure with a high aspect ratio (12) and high resolution (sub 30 nm).

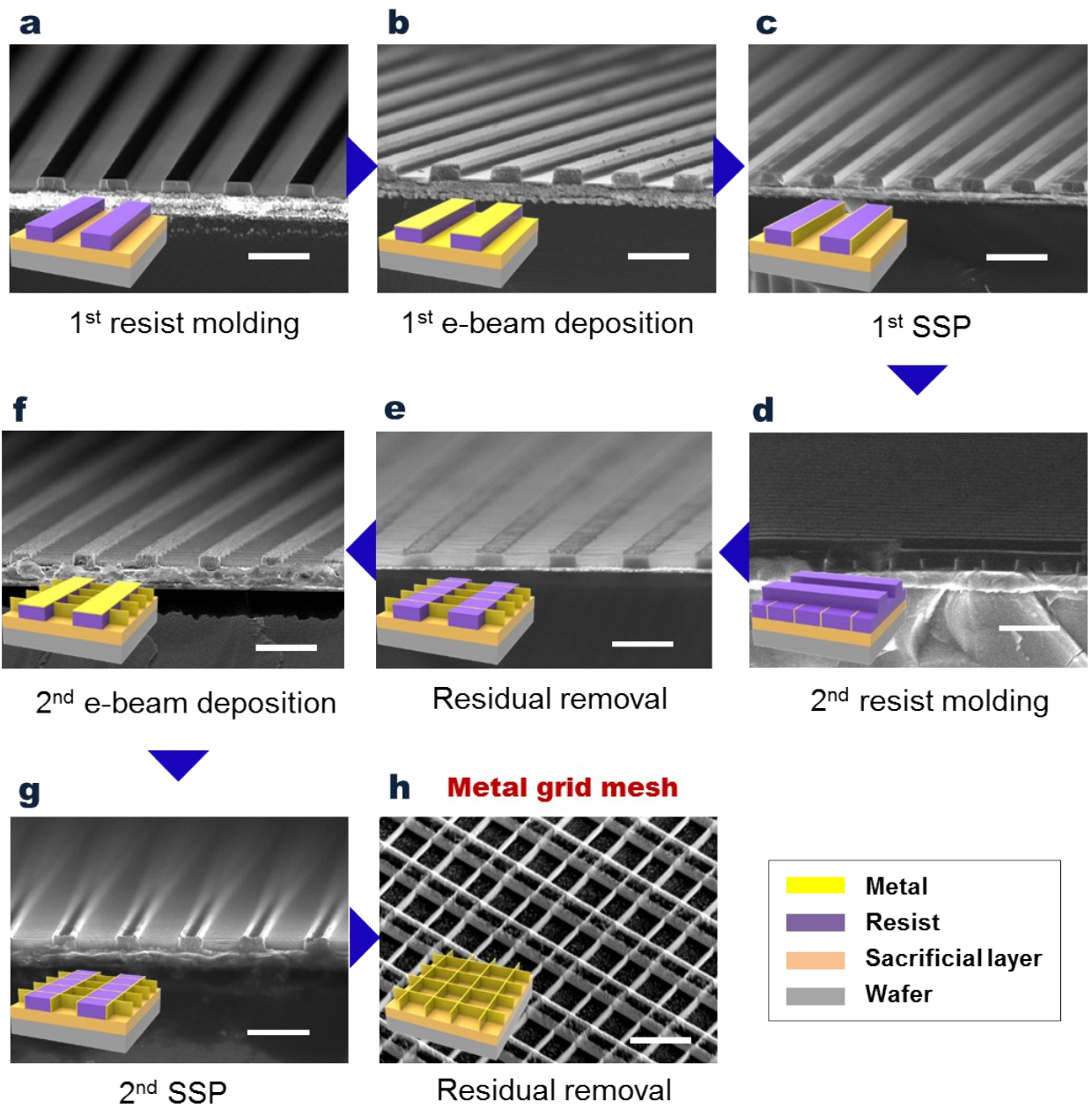


Figure S2. Schematic diagrams of specific fabrication steps and SEM images of the high aspect ratio metal grid mesh.

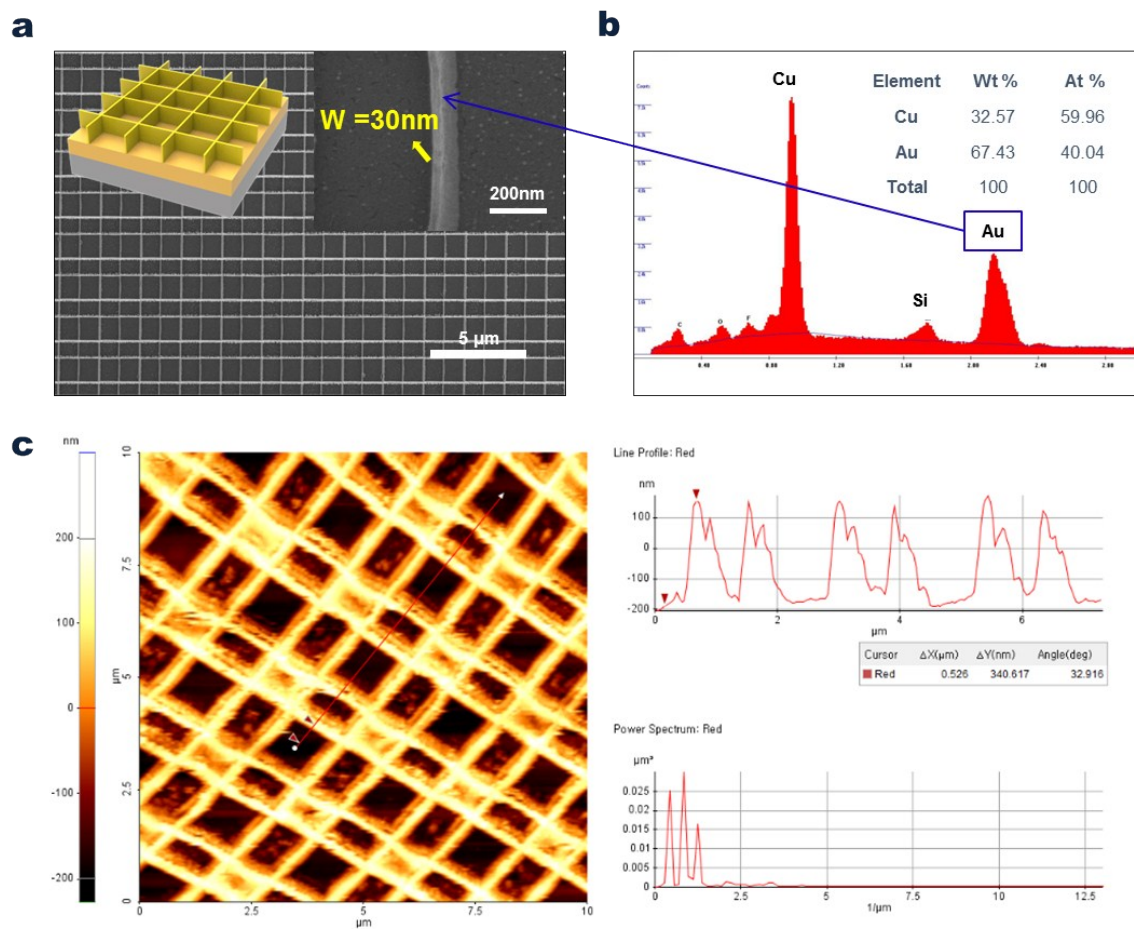


Figure S3. Confirmation of resolution ($\sim 30\text{nm}$), material and height ($\sim 350\text{nm}$) of Au grid mesh by SEM(a), EDAX analysis(b), and AFM(c), respectively.

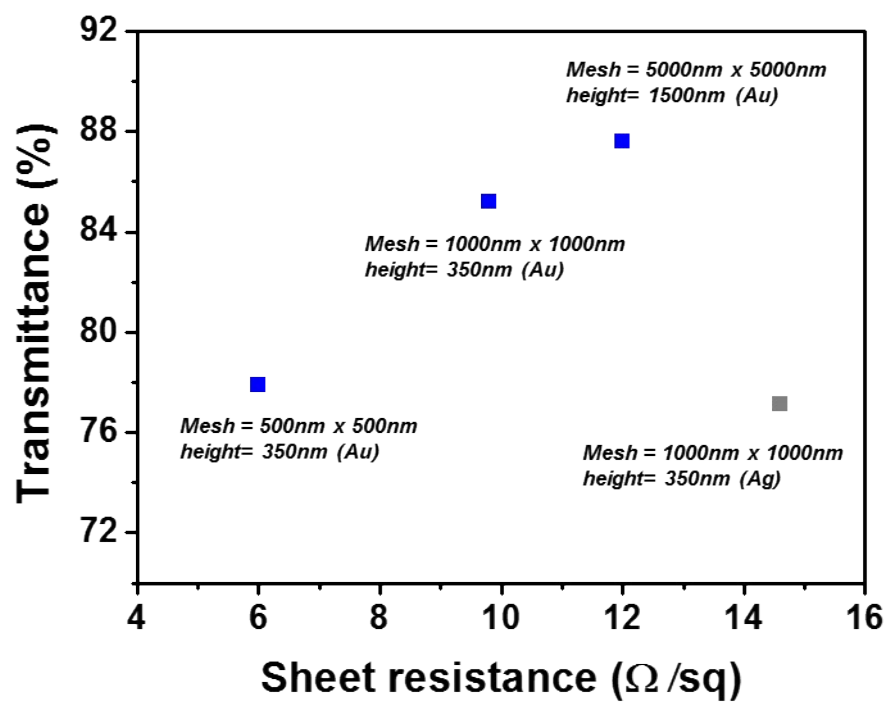


Figure S4. Transmittance at 550nm and sheet resistance at different metal grid mesh structure.

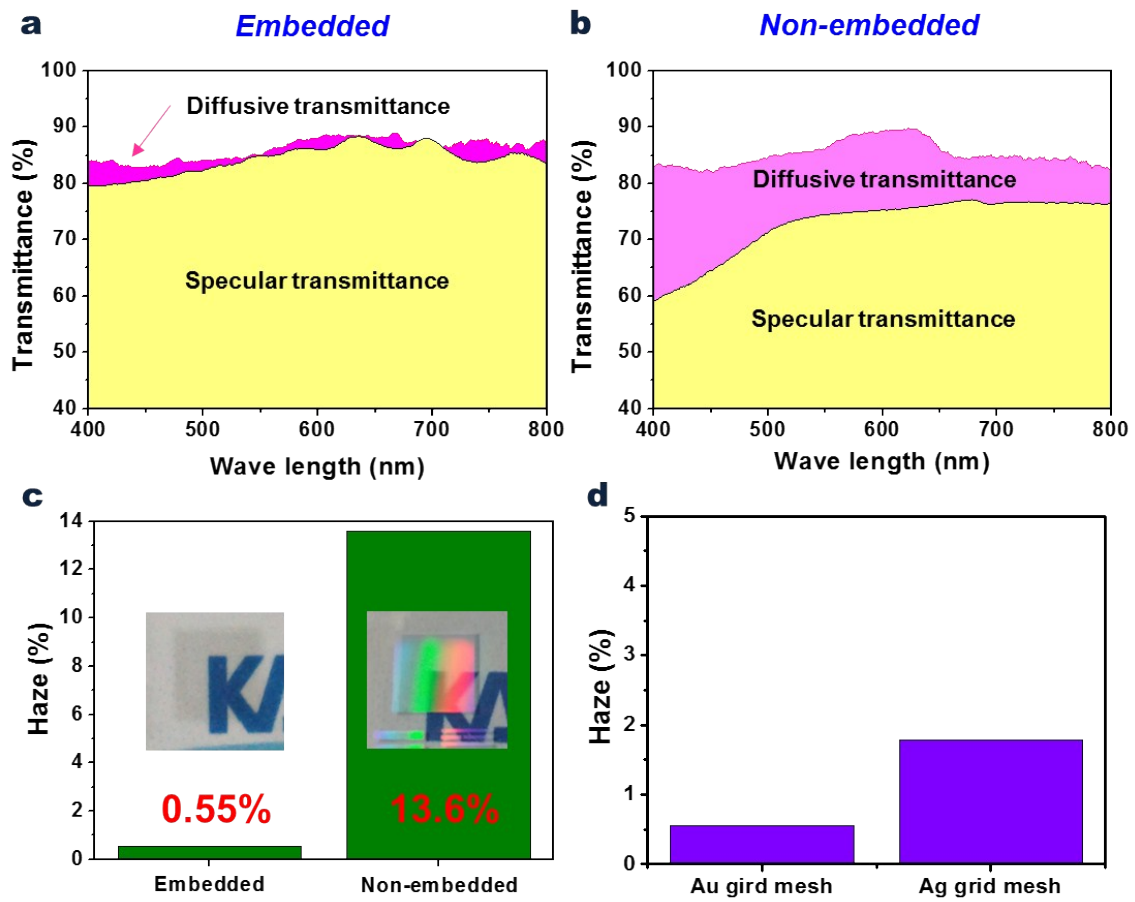


Figure S5. Diffusive and specular transmittances of the substrate-embedded metal grid mesh electrode (a) and the non-embedded Au grid mesh electrode (b) in the visible wavelength region and the characterization of the haze of the Au grid mesh electrode (c) and the Ag grid mesh electrode (d).

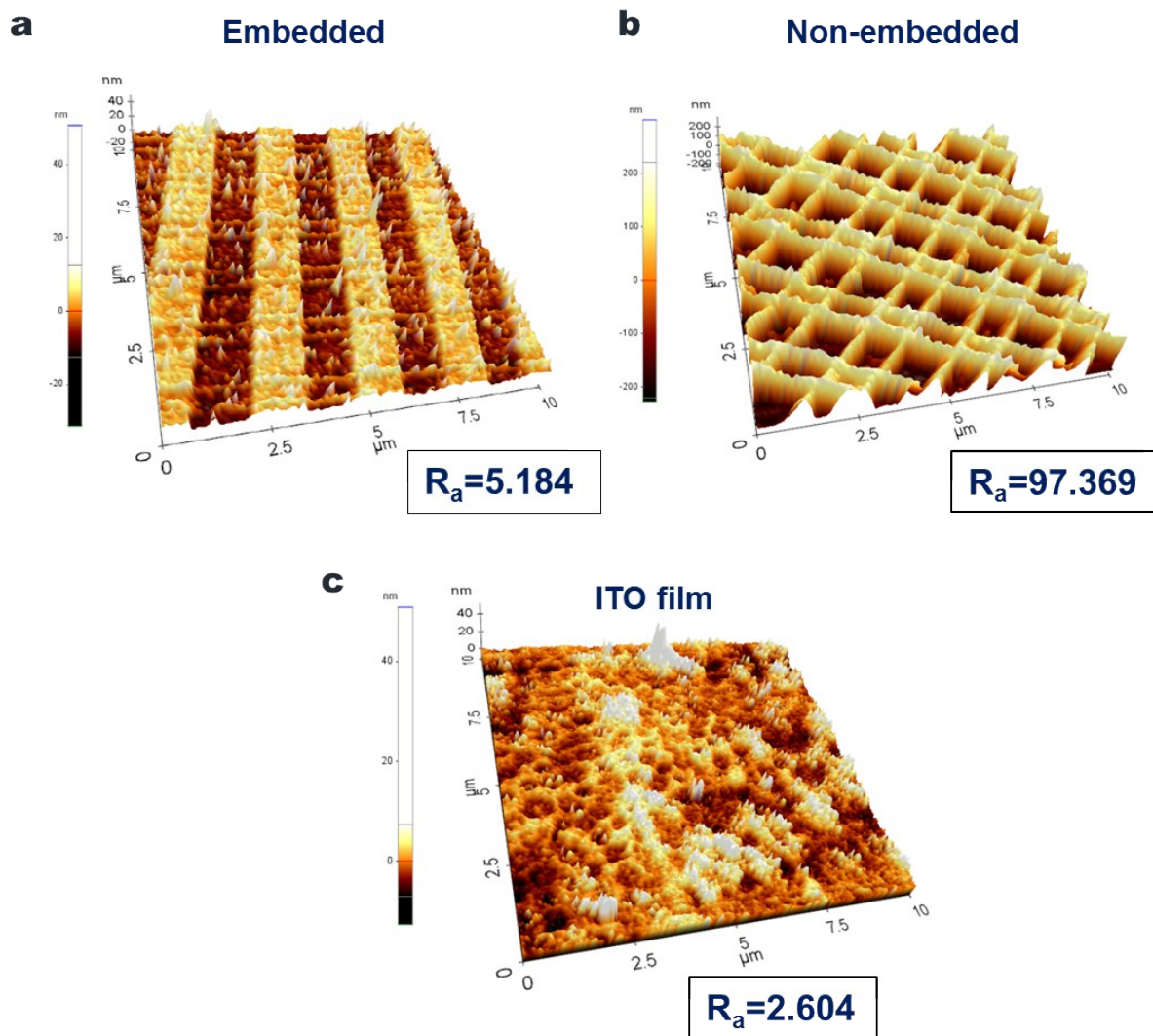
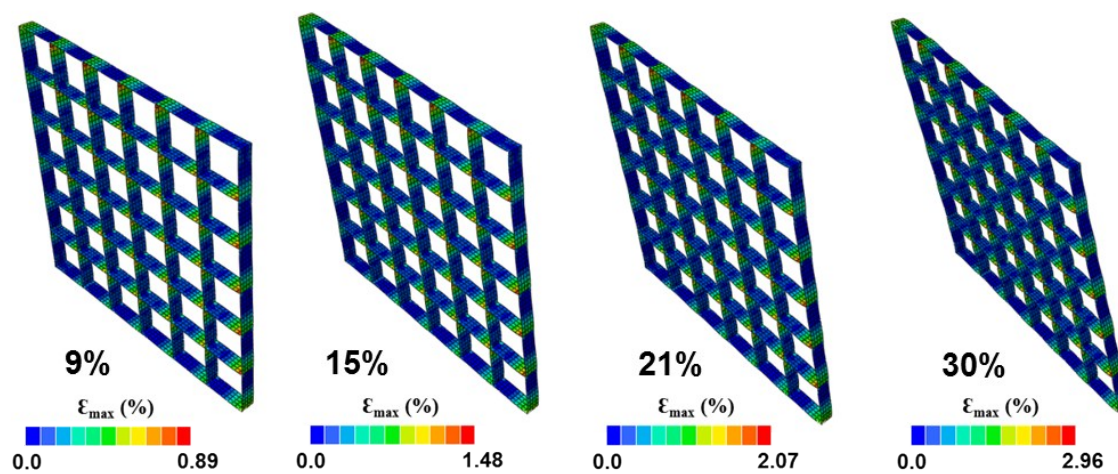


Figure S6. AFM topography results for the substrate-embedded metal grid mesh transparent electrode (a), non-embedded metal grid mesh (b), and ITO film (c), respectively.

a Diagonal stretching



b Orthogonal stretching

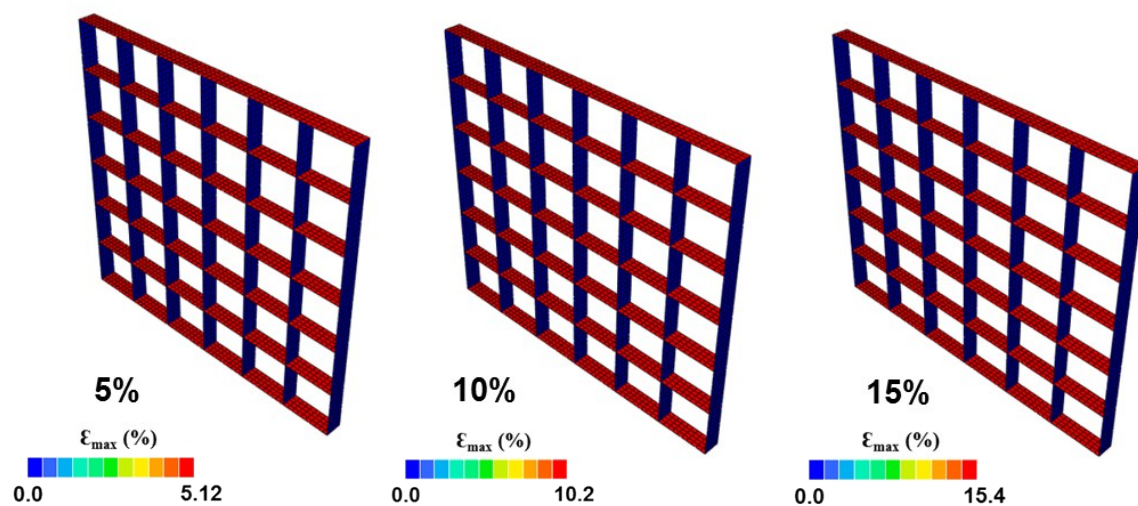


Figure S7. The relationship between stretching direction and maximum principal strain for a metal grid mesh structure according to FEM simulations. (a) Diagonal stretching and (b) orthogonal stretching of Au grid mesh structures with maximum principal strain localization.

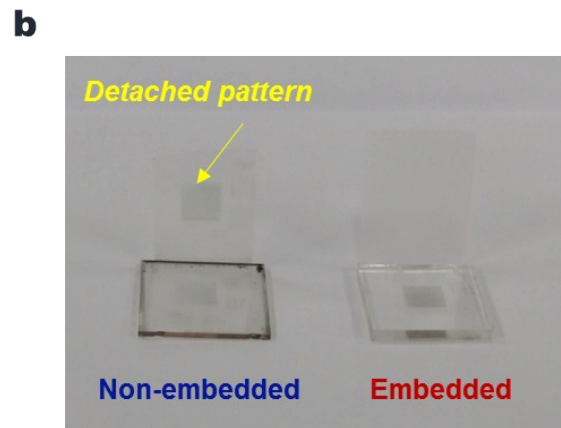
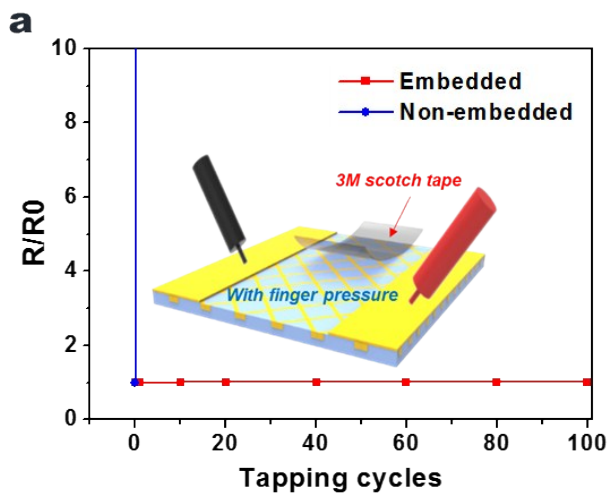


Figure S8. Mechanical adhesion stability. (a) The resistances of metal grid mesh embedded in soft substrate and metal grid mesh on a glass substrate during repeated taping cycles. (b) Photographs of mesh samples after repeated tapping cycles (3M scotch tape) with finger pressure force.